

High concentrations of a passive scalar in turbulent dispersion

NILS MOLE¹, THOMAS P. SCHOPFLOCHER²
AND PAUL J. SULLIVAN²

¹Department of Applied Mathematics, University of Sheffield, Hicks Building,
Sheffield S3 7RH, UK

²Department of Applied Mathematics, The University of Western Ontario, London N6A 5B7,
Ontario, Canada

(Received 7 March 2007 and in revised form 29 February 2008)

In problems involving the dispersion of hazardous gases in the atmosphere, the distribution of high concentrations is often of particular interest. We address the modelling of the distribution of high concentrations of a dispersing passive scalar at large Péclet number, concentrating on the case of steady releases. We argue, from the physical character of the small-scale processes, and from the statistical theory of extreme values, that the high concentrations can be fitted well by a Generalized Pareto Distribution (GPD). This is supported by evidence from a range of experiments. We show, furthermore, that if this is the case then the ratios of successive high-order absolute moments of the scalar concentration are linearly related to the reciprocal of the order. The linear fit thus obtained allows the GPD parameters to be determined from the moments. In this way the moments can be used to deduce the properties of the high concentrations, in particular the maximum possible concentration $\theta_{\max} = \theta_{\max}(\mathbf{x})$. We argue, on general physical grounds, that θ_{\max}/C_0 (where $C_0 = C_0(X)$ is the centreline mean concentration, and X is the downstream distance from the source) decreases to zero very far from the centreline, but that the decrease takes place on a length scale much larger than the mean plume width (because it is controlled by the relatively slowly acting molecular diffusion, rather than the fast turbulent advection). Thus, over the distances for which accurate measurements can be made, we expect θ_{\max}/C_0 to be approximately constant throughout the plume cross-section. On the centreline, we argue that θ_{\max}/C_0 increases downstream from the source, reaches a maximum and then decreases, ultimately tending to 1 far downstream. In support of these deductions we present results for some high-quality data for a steady line source in wind tunnel grid turbulence. Finally, we apply to this problem some existing models for the relationships between moments. By considering the behaviour far from the centreline in these models, and linking the moments to the high concentrations, we derive relationships between the model parameters. This allows us to derive an expression for θ_{\max}/C_0 which depends on a total of 5 parameters, and (weakly) on C/C_0 (where $C = C(\mathbf{x})$ is the local mean concentration). Comparison with the data is encouraging. We also discuss possible methods for modelling the spatial variation of these 5 parameters.

1. Introduction

The dispersion of a passive scalar in a turbulent flow is governed by two fundamental physical processes: advection by the turbulent velocity field, and

molecular diffusion. Most turbulent flows in environmental and engineering applications have large Péclet number $Pe = ul/\kappa$, where u and l are appropriate velocity and length scales for the turbulent fluctuations, and κ is the molecular diffusivity. In this case turbulent advection acts on a much faster time scale than molecular diffusion, the ratio of the time scales being given by Pe if the length scales for the velocity and concentration fields are comparable: see the Appendix for some more detailed arguments about the time scales. Advection acts to stretch the scalar cloud or plume out into thin sheets and strands (Batchelor 1952), as observed experimentally (Dahm, Southerland & Buch 1991; Corriveau & Baines 1993; Buch & Dahm 1996, 1998). Although molecular diffusion is a much slower process, it is nevertheless a vital one: it is the only means by which the scalar concentration can be altered, and it limits the smallest scales which can be present in the scalar field. For Schmidt number ν/κ of order 1 or greater this smallest scale is of the order of the conduction cutoff length $\lambda_c = (\nu\kappa^2/\epsilon)^{1/4}$ (Batchelor 1959), where ν is the kinematic viscosity and ϵ is the turbulent energy dissipation rate per unit mass. Molecular diffusion also has the effect of dissipating the variance and higher moments of the concentration (Batchelor 1959; Chatwin & Sullivan 1979, 1990*b*).

In practical problems, for example that of assessing the hazards associated with accidental releases of toxic or flammable gases, it is desirable to know the temporal and/or spatial variation of the concentration moments and, ideally, of the probability density function (p.d.f.) of concentration. Often it is the high concentration tail of the p.d.f. which is of particular interest, especially for toxic gases for which high concentrations tend to be disproportionately harmful (see e.g. ten Berge, Zwart & Appelman 1986; Davies 1989; Griffiths 1991). Legal regulations governing such gases are often expressed in terms of high concentrations; for example, in the UK the Control of Substances Hazardous to Health Regulations 2002 impose short-term workplace exposure limits on the concentrations of many hazardous gases. (For a full assessment of the hazards, further information such as the spatial and temporal scale and structure of high concentrations, and the response characteristics of the exposed organism, would also be required.)

Chatwin & Sullivan (1990*a*) exploited the very different time scales of advection and diffusion to suggest a simple framework for the central moments of concentration. They argued that, since diffusion is a slow process, the structure of the moments will be close to that in the absence of molecular diffusion. For a uniform concentration source, the only possible concentrations in the absence of diffusion are zero and the source concentration θ_1 . The p.d.f. of concentration can then be written as

$$p(\theta) = (1 - \pi)\delta(\theta) + \pi\delta(\theta - \theta_1),$$

where $\pi(x, t)$ is the probability of being in the source fluid and δ is the Dirac delta function. The mean concentration $C(\mathbf{x}, t) = E\{\Gamma(\mathbf{x}, t)\}$, where Γ is the concentration and $E\{\cdot\}$ denotes the expected value, or ensemble mean, is then given by

$$C = (1 - \pi) \int \theta \delta(\theta) d\theta + \pi \int \theta \delta(\theta - \theta_1) d\theta = \pi\theta_1,$$

and the n th central moment

$$\mu_n(\mathbf{x}, t) = E\{[\Gamma(\mathbf{x}, t) - C(\mathbf{x}, t)]^n\}$$

is given by

$$\begin{aligned} \mu_n &= (1 - \pi) \int (\theta - C)^n \delta(\theta) d\theta + \pi \int (\theta - C)^n \delta(\theta - \theta_1) d\theta \\ &= (1 - \pi)(-C)^n + \pi(\theta_1 - C)^n. \end{aligned}$$

Hence

$$\frac{\mu_n}{\theta_1^n} = \frac{C}{\theta_1} \left(1 - \frac{C}{\theta_1}\right)^n + (-1)^n \left(1 - \frac{C}{\theta_1}\right) \left(\frac{C}{\theta_1}\right)^n. \tag{1.1}$$

Essentially, Chatwin & Sullivan (1990a) proposed that well downstream in self-similar turbulent flows (1.1) could be modified to take account of the effect of molecular diffusion. This was done, firstly, by replacing the source concentration θ_1 by a representative local value αC_0 , where α is a constant and C_0 is the centreline mean concentration. Secondly, a constant of proportionality β^n was introduced to take account of dissipation and of the increased background concentration resulting from diffusion out of the sheets and strands of high concentration:

$$\frac{\mu_n}{(\alpha C_0)^n} = \beta^n \{ \hat{C}(1 - \hat{C})^n + (-1)^n (1 - \hat{C})\hat{C}^n \}, \tag{1.2}$$

where

$$\hat{C} = \frac{C}{\alpha C_0}.$$

Because of dissipation, β would be expected to be less than 1. Chatwin & Sullivan (1990a) found that observations from a number of experiments could be fitted well by (1.2) with a constant value of α , and β approximately constant in the cross-stream direction.

When considering higher moments of concentration, and associated p.d.f.s, it is often useful to consider normalized moments, in particular the skewness K_3 , kurtosis K_4 and higher-order equivalents K_n , defined by

$$K_n = \frac{\mu_n}{\mu_2^{n/2}} \quad \text{for } n = 3, 4, \dots \tag{1.3}$$

Mole & Clarke (1995) showed that (1.2) implies that

$$K_4 = K_3^2 + 1, \quad K_5 = K_3^3 + 2K_3, \tag{1.4}$$

and gave a general expression for K_n as a function of K_3 . They analysed experimental data from a steady release close to the ground in the field, and suggested that (1.4) should be replaced by

$$K_4 = a_4 K_3^2 + b_4, \quad K_5 = a_5 K_3^3 + b_5 K_3, \tag{1.5}$$

where a_4 , b_4 , a_5 and b_5 are constants. This formulation has been shown to hold to a good approximation in a variety of experiments, including plumes in atmospheric boundary layers under various stability classes (Mole & Clarke 1995; Lewis, Chatwin & Mole 1997), clouds in the wind tunnel with varying density and with different forms of fence (Chatwin & Robinson 1997), and plumes in wind tunnels (Schopflocher & Sullivan 2005; Schopflocher, Smith & Sullivan 2007).

Sawford & Sullivan (1995) argued that (1.2) would describe the lateral moment structure, with α and β varying with time for an instantaneous release, or with downstream distance for a steady release. They also generalized (1.2) to the case of

non-uniform source concentration by introducing additional parameters λ_n for $n \geq 3$:

$$\left. \begin{aligned} \frac{\mu_2}{(\alpha\beta C_0)^2} &= \hat{C}(1 - \hat{C}), \\ \frac{\mu_3}{(\alpha\beta C_0)^3} &= \hat{C}(\lambda_3^2 - 3\hat{C} + 2\hat{C}^2), \\ \frac{\mu_4}{(\alpha\beta C_0)^4} &= \hat{C}(\lambda_4^3 - 4\lambda_3^2\hat{C} + 6\hat{C}^2 - 3\hat{C}^3), \\ &\vdots \end{aligned} \right\} \quad (1.6)$$

If $\lambda_n = 1$ for all n then (1.6) reduces to (1.2). As with α and β , the λ_n could be expected to vary in time for an instantaneous release, or with downstream distance for a steady release. Sawford & Sullivan (1995) fitted these parameters to data from a steady line source experiment in wind tunnel grid turbulence (Sawford & Tivendale 1992), finding that they varied very slowly with downstream distance (see Table 1 of Schopflocher *et al.* (2007)). Similarly, we would expect the parameters a_4, b_4, a_5, b_5 and higher-order equivalents to be approximately constant in the cross-stream direction, but to vary slowly with time or downstream distance. This has been confirmed for the Sawford & Tivendale (1992) experiments by Schopflocher & Sullivan (2005) and Schopflocher *et al.* (2007). Schopflocher & Sullivan (2005) also showed that the expression for K_4 in (1.5) followed approximately from (1.6). The relationships between the moments predicted by Chatwin & Sullivan (1990a) and Sawford & Sullivan (1995) have been found to agree reasonably well with measurements from a range of experiments, including jets, wakes, plumes, uniformly sheared flow and buoyant jets (Chatwin & Sullivan 1990a; Moseley 1991; Sawford & Sullivan 1995; Ye 1995).

In this paper, we argue that β is principally a measure of the dissipation accomplished by molecular diffusion, tending to zero in the limit of infinite diffusion time, and that we do not, therefore, expect β to be constant across the whole plume cross-section. Any source material arriving far from the centreline will have taken a long time to get there, because of the large distance involved. It will, therefore, have been acted on by diffusion for a long time, so we expect that β will tend to zero far from the centreline. However, the length scale on which β decreases will be much greater than that on which the mean concentration C decreases, since the latter is dominated by the much faster advection. Where C becomes very small, it is usually difficult to obtain reliable measurements, so we expect *measured* values of β to be approximately constant in the cross-stream direction over the range of distances for which measurements are made, consistent with the results described above.

The framework outlined above provides a simple description of the moments, enabling estimates to be made of higher moments given knowledge of the mean concentration. Given the first few moments, estimates can be made of the p.d.f. (see e.g. Derksen & Sullivan 1990). However, while such an approach may well give a good approximation to the bulk of the p.d.f., it will not necessarily give good results for the high concentration tail. The main aim of the present paper is to utilize the above framework to derive results for this tail, in particular for the maximum possible concentration. Away from the source, the latter will always be less than the largest source concentration, because of molecular diffusion.

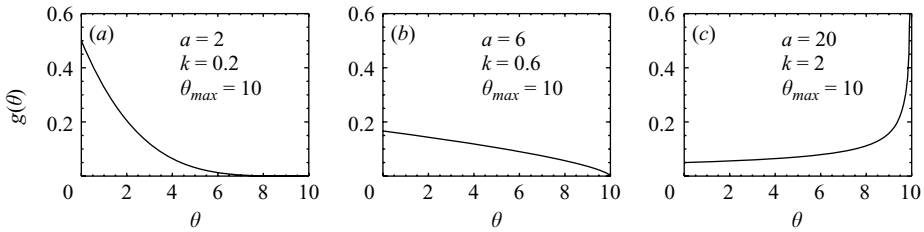


FIGURE 1. Examples of the possible GPD shapes.

As described above, the turbulent velocity field stretches the cloud or plume out into thin sheets or strands. These become thin enough for molecular diffusion to act strongly across them, so they cannot become thinner than the conduction cutoff. The lower-concentration part of the p.d.f. is dominated by concentrations in fluid which does not emanate from the source, and into which scalar has diffused from source fluid. The high-concentration tail of the p.d.f., on the other hand, represents the concentration in the thin sheets and strands which contain most of the source fluid, and which are relatively rare, except very close to the source or soon after release. Since these sheets and strands are controlled by the balance between the local stretching by the velocity field, and molecular diffusion across them, we might expect the tail of the concentration p.d.f. to have a universal character, regardless of the details of the larger scale flow. Further support for such universality is provided by statistical extreme value theory (see e.g. Kristensen, Weil & Wyngaard 1989; Lewis & Chatwin 1995*b*; Mole *et al.* 1995; Anderson, Mole & Nadarajah 1997; Munro, Chatwin & Mole 2001; Schopflicher 2001; Schopflicher & Sullivan 2002 for previous applications to turbulent dispersion). In particular, this theory shows that (Pickands 1975), under certain regularity conditions, the distribution of a random variable, conditional on being above a high threshold value, can be approximated by the Generalized Pareto Distribution (GPD), which has the p.d.f.

$$g(\theta) = \frac{1}{a} \left(1 - \frac{k\theta}{a} \right)^{1/k-1}, \quad (1.7)$$

where k and a are parameters, with a positive. Since in turbulent dispersion there is a finite maximum possible concentration we expect that, when applied to concentration in the present context, k will also be positive, with (1.7) then being valid for

$$0 \leq \theta \leq \theta_{\max},$$

where

$$\theta_{\max} = \frac{a}{k} < \theta_2,$$

θ_2 being the largest source concentration. The parameter k determines the shape of $g(\theta)$. For $0 < k < 1/2$, $g(\theta)$ is zero and has zero gradient at $\theta = \theta_{\max}$; for $1/2 < k < 1$ it is zero at $\theta = \theta_{\max}$ but has infinite gradient there; while for $k > 1$, $g(\theta)$ is unbounded at $\theta = \theta_{\max}$. Examples of these three shapes are given in figure 1. In general we expect a , k and θ_{\max} to depend on temporal and spatial location.

We also expect dependence of the high-concentration tail on the Reynolds number $Re = ul/\nu$ and Péclet number $Pe = ul/\kappa$. A simple illustration of this is provided by the conduction cutoff length $(\nu\kappa^2/\epsilon)^{1/4}$, at which scale diffusion acts strongly and we expect the largest concentrations to be found, which is proportional to $Re^{-1/4}Pe^{-1/2}$. So we expect the tail to be GPD, but the parameters to depend on Re and Pe . In

the Appendix we give some arguments suggesting that θ_{\max}/C_0 will typically be an increasing function of Re and Pe .

The main aim of this paper is to use (1.5), (1.6) and (1.7) to derive expressions for the parameters governing high concentrations, thus providing a relatively simple way of describing and modelling high concentrations. In §2 we show that the ratio of successive high-order absolute moments can be expressed as a linear function of the reciprocal of the order n , and that this enables the identification of the GPD parameters a , k and θ_{\max} from experimental data. In §3 we show that applying (1.5) and (1.6) in the periphery of a plume gives a relationship between the a_n and the λ_n . Combining this with the result of §2, we derive expressions for a , k and θ_{\max} in terms of α , β , λ_3 , a_4 and a_5 , and compare them with the line source, grid turbulence, data of Sawford & Tivendale (1992).

2. Estimating properties of the distribution of high concentrations from data

2.1. Experimental data

The experimental data we shall use are those of Sawford & Tivendale (1992) for a steady line source in wind tunnel grid turbulence. The experimental details are given in Sawford & Tivendale (1992), and Sawford & Sullivan (1995) repeat some of these details, as well as presenting further analysis of the data (for example of the first few moments of concentration). Here we summarize the main experimental details.

The measurements were made in a suction wind tunnel with a rectangular test section 0.69 m high, 1.07 m wide and 3.3 m long. Turbulence was generated with a planar ‘punched plate’ grid with circular holes of diameter 0.0208 m in a hexagonal pattern. The mesh length (i.e. hole spacing) was $M = 2.54 \times 10^{-2}$ m, giving a solidity ratio of 0.39. The source was a horizontal heated Nichrome wire of diameter $d = 0.213$ mm placed a distance $x_0 = 12.2M$ downstream of the grid. The mean air speed was $U = 5.0$ m s⁻¹, with a corresponding Reynolds number UM/ν of 8500, where ν is the kinematic viscosity of unheated air (1.5×10^{-5} m² s⁻¹ at 20°C).

Temperature fluctuations were measured with a platinum cold wire 1.27 μm in diameter and 0.4 mm long. The temperature signal was low-pass filtered at 2 kHz and sampled at 4096 Hz. Statistics were calculated from 20 separate 1 s samples, i.e. from a total of 81920 points. Sawford & Sullivan (1995) reported that frequencies up to 1 kHz accounted for about 90 % of the temperature variance near the source, and over 99 % of the variance far downstream.

The mean temperatures near the source were up to 50 K above background, similar to the experiments of Stapountzis *et al.* (1986), but much higher than in Warhaft (1984). Sawford (2004) showed that, as a result, an enhanced diffusivity is required to fit the data in the near field. Sawford (2004) also showed that the intensity of fluctuations is reduced by comparison with the Warhaft data, but that in the far field these source effects become unimportant. Note that figure 3(a) of Sawford & Sullivan (1995) shows that in the near field α is smaller for the Sawford & Tivendale data than for the Warhaft data, but that in the far field the values are similar, while the β values are comparable.

2.2. A moment-based method for fitting high concentrations

As outlined above, we expect that the GPD given by (1.7) will give a good approximation to the high-concentration tail of the p.d.f. We want to identify the parameters a , k and θ_{\max} , and, in general, find their temporal and spatial variation.

A number of methods have been applied previously to estimating these parameters from data. These fall broadly into two categories.

One approach is to fit the GPD to concentration values above some high threshold, using a method such as maximum likelihood estimation to carry out the fitting. This approach was used by Mole *et al.* (1995), Anderson *et al.* (1997), Schopflicher (2001) and Munro *et al.* (2001), providing confirmation of the good fit provided by the GPD. This approach has the advantage of using only the high values of concentration which are expected to be fitted well by the GPD, and avoiding problems at low concentration levels caused by noise or uncertain baseline (see Lewis & Chatwin 1995*a*). Drawbacks are that some subjectivity is involved in choosing the threshold, and that it does not lend itself to being incorporated into a physical model.

The other approach is to fit a p.d.f. to all the data. Usually this p.d.f. comprises a mixture of a GPD or equivalent, to capture the high-concentration behaviour, with another p.d.f. designed to capture the behaviour of the bulk of the concentration values. Examples are a mixture of GPD and exponential distribution (Lewis & Chatwin 1995*b*, 1997), and a mixture of GPD and beta distribution (Munro, Chatwin & Mole 2003*a*). This approach has the disadvantages of being influenced by any problems with the data at small concentrations, and of the fitting not being specifically tailored to the high concentrations. It is also not straightforward to use it in a physical model.

Here we choose instead to use a method based on moments. Advantages of this are that it is simple, and that it is easier to produce physical models for the moments than for the p.d.f. itself. Furthermore, the experimental record lengths (or number of realizations for a non-steady release) required to obtain good estimates of the first few moments that we use are small compared with those needed to capture rare events in the tails. (In effect we are extrapolating from the first few moments to the very high moments which correspond to behaviour in the tail, using the assumption that the tail is described by the GPD.) This is particularly relevant to field experiments, where long experiments are affected by the inherent non-stationarity of the flow.

First we write the p.d.f. of concentration, $p(\theta)$, as

$$p(\theta) = (1 - \eta)f(\theta) + \eta g(\theta) \quad \text{for } 0 \leq \theta \leq \theta_{\max}, \quad (2.1)$$

where $g(\theta)$ is the GPD given by (1.7) and η is a positive constant, and we assume that at high concentrations (i.e. as $\theta \rightarrow \theta_{\max}$) $f(\theta)$ is insignificant so $p(\theta) \approx \eta g(\theta)$. If we let θ_c be the concentration above which $p(\theta) \approx \eta g(\theta)$, then the probability that $\theta > \theta_c$ is approximately equal to A , where A is defined by

$$A = \eta \int_{\theta_c}^{\theta_{\max}} g(\theta) d\theta = \eta \left(1 - \frac{\theta_c}{\theta_{\max}}\right)^{1/k}. \quad (2.2)$$

Although superficially (2.1) has the form of a mixture of p.d.f.s f and g , in general this will not be the case. This is because $p(\theta) \approx \eta g(\theta)$ at large θ , allowing the possibility of $\eta > 1$, and at smaller θ it is possible to have $p(\theta) < \eta g(\theta)$, in which case $f(\theta)$ could be negative, and thus not a p.d.f. If we wish we can rewrite (2.1) as an approximate mixture of p.d.f.s by splitting $p(\theta)$ into the parts above and below θ_c .

We now define the absolute moments m_n by

$$m_n = E \{ \Gamma^n \} = \int_0^{\theta_{\max}} \theta^n p(\theta) d\theta, \quad (2.3)$$

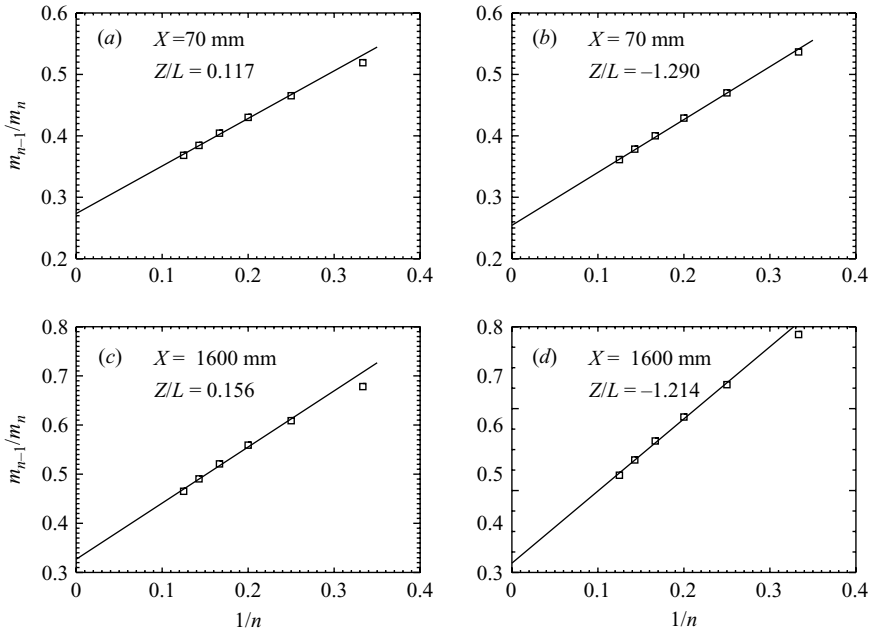


FIGURE 2. Linear fits to the moment ratios for data from Sawford & Tivendale (1992). X is the downstream distance from the source, Z is the cross-stream distance from the centreline, and L is the mean plume width.

and use (2.1) to obtain

$$\begin{aligned}
 m_n &= (1 - \eta) \int_0^{\theta_{\max}} \theta^n f(\theta) \, d\theta + \eta \int_0^{\theta_{\max}} \theta^n g(\theta) \, d\theta \\
 &\approx (1 - \eta) \int_0^{\theta_c} \theta^n f(\theta) \, d\theta + \eta \int_0^{\theta_{\max}} \theta^n g(\theta) \, d\theta.
 \end{aligned}$$

For sufficiently large n the contribution from f will be small compared with that from g . Thus

$$m_n \approx \eta \int_0^{\theta_{\max}} \theta^n g(\theta) \, d\theta. \tag{2.4}$$

For $g(\theta)$ given by (1.7), with parameters a and k , we have

$$\int_0^{\theta_{\max}} \theta^n g(\theta) \, d\theta = \frac{n! a^n}{(1+k)(1+2k)\cdots(1+nk)}. \tag{2.5}$$

Thus, for sufficiently large n ,

$$\frac{m_{n-1}}{m_n} \approx \frac{1+nk}{na} = \frac{1}{a} \left(\frac{1}{n} \right) + \frac{k}{a}. \tag{2.6}$$

So at high-order n we expect the ratio of successive moments to be linear in $(1/n)$, and a linear fit should yield the values of a and k , and of $\theta_{\max} = a/k$. Equation (2.4) can then be used to find η .

Figure 2 shows plots of m_{n-1}/m_n against $1/n$ for the steady line source, grid turbulence, data of Sawford & Tivendale (1992). X is the downstream distance from the source, Z is the cross-stream distance from the centreline, and L is the mean

plume width. The latter is measured as one standard deviation in the cross-stream profile of C , which is very close to Gaussian (Sawford & Sullivan 1995). In all cases, including those not shown here, we found a good linear fit down as far as $n=4$ (and usually a reasonable approximation was achieved as far as $n=3$). We identified the best-fit GPDs by a least-squares fit of (2.6) to the moment ratios for $n=4$ to 8.

Figure 3 shows corresponding measured p.d.f.s of θ/C_0 (i.e. $C_0p(\theta)$), with the best fit GPDs superimposed. As can be seen, the GPD contribution $\eta g(\theta)$ gives a reasonable approximation to $p(\theta)$ over a considerable range of concentration values. We estimate the concentration θ_c , above which this is the case, by choosing θ_c such that

$$|\eta g(\theta) - p(\theta)| < \frac{1}{40C} \quad \text{for } \theta \geq \theta_c.$$

In this criterion, we scale the absolute difference by the mean concentration C , to achieve comparability between different cases. Other possibilities, like scaling the difference by $p(\theta)$, lead to problems when $p(\theta)$ becomes small in the tail. Of the various dimensionally correct scalings one could choose, C seems likely to give the most robust and sensible results. We tried a range of different numerical factors, and chose 40 since it appeared to give the best balance between making θ_c too large or too small, across the range of spatial positions. The resulting values of θ_c are indicated in figure 3 by the dashed lines. Figure 4 shows the percentage of the concentration range $[0, \theta_{\max}]$ which lies above θ_c , and the percentage of the area (given by (2.2)) under this part of the p.d.f. Here, for the centreline, we use the closest measuring station to the centreline at each downstream distance. These stations have $Z/L \lesssim 0.2$. On the centreline the GPD accounts for about 40% of the range, and a little under 10% of the area. At about $1L$ from the centreline the GPD accounts for about 80% of the range and 20% of the area. So although the concentrations which are fitted well by the GPD occur relatively rarely, they form a substantial proportion of the whole concentration range.

θ_{\max} ought to be larger than the largest measured concentration Γ_{\max} , but in some cases, particularly for larger values of k , i.e. for shorter tails, the estimated maximum $\hat{\theta}_{\max}$ is slightly less than Γ_{\max} . Munro *et al.* (2001) found that fitting a GPD to high concentrations using maximum likelihood gave $\hat{\theta}_{\max}/\Gamma_{\max}$ always greater than 1, with values up to about 4, but mostly less than 1.5. However, they also used a method based on linear fits to mean excess plots, and this method did sometimes give $\hat{\theta}_{\max} < \Gamma_{\max}$. In our case, the points shown in figure 2, and also those for the cases not shown, show a suggestion of a slight curvature, with increasing gradient as n increases. This means that we may well have underestimated θ_{\max} in some cases. However, since the error in estimating moments from the measurements increases with n , we cannot establish this with real confidence.

Physical arguments for the variation of the GPD parameters of greatest interest, i.e. a , k and θ_{\max} , are discussed in the next section, and their observed values are discussed in §2.4. The centreline variation of the other parameter, η , is illustrated in figure 5. In applying (2.4) to calculate η we found that there was little variation in the values obtained from $n=3$ upwards, and here we have used the value obtained for $n=4$. Initially η decreases with downstream distance, before reaching a minimum and then increasing gradually downstream. The cross-stream variation of η is discussed in §2.4.

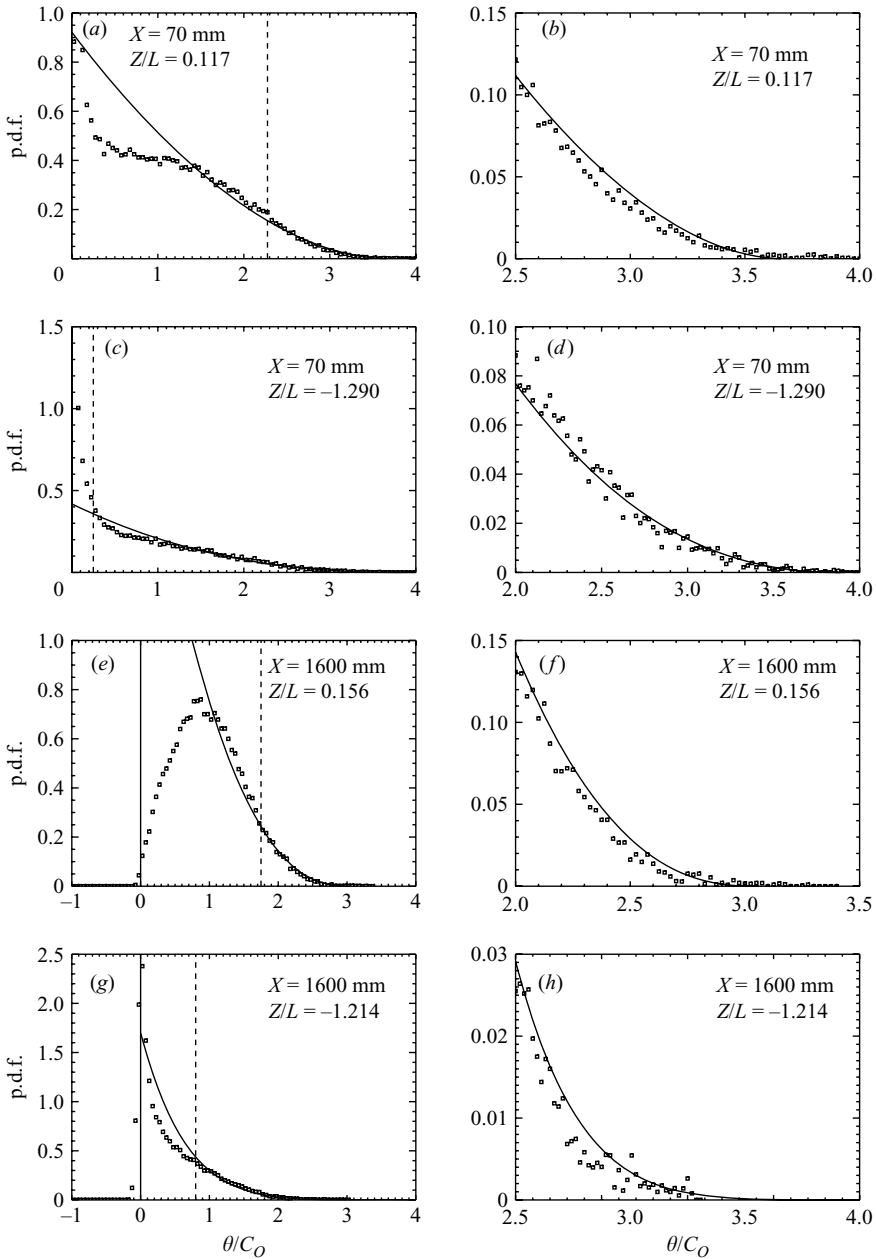


FIGURE 3. The measured p.d.f. of θ/C_0 (points), and GPD for fitted k and a values (curves). The right-hand panels show blow-ups of the tails. The dashed lines mark the estimated values of θ_c/C_0 .

2.3. The spatial variation of the GPD parameters: physical arguments

For the rest of this paper we concentrate on the case of a steady line source, and compare our results with the experimental measurements of Sawford & Tivendale (1992) for grid turbulence. Many of the principles will also apply, with little modification, to steady point sources and instantaneous cloud releases. Before

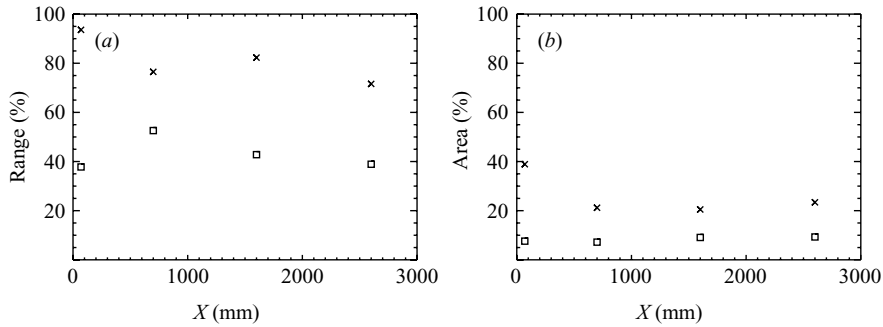


FIGURE 4. Variation with downwind distance X of the percentage range and area accounted for by the GPD, i.e. by $\theta \geq \theta_c$. (a) Range $1 - \theta_c/\theta_{\max}$, (b) area A . The squares represent centreline measurements, and the crosses measurements at about $1L$ from the centreline.

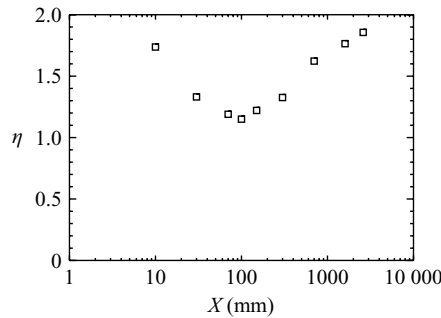


FIGURE 5. Variation of centreline η with downstream distance X .

examining the behaviour of the fitted GPD parameters for these measurements, we give physical arguments for the behaviour we would expect to find.

On the centreline, very close to the source we expect that θ_{\max} will tend to the largest source concentration θ_2 , and that the centreline mean concentration C_0 will tend to the mean source concentration θ_1 . Thus, as $X \rightarrow 0$ we have

$$\frac{\theta_{\max}}{C_0} \rightarrow \begin{cases} \frac{\theta_2}{\theta_1} (> 1) & \text{non-uniform source,} \\ 1 & \text{uniform source.} \end{cases}$$

Away from the source, but still close to it, molecular diffusion will have little effect, so θ_{\max} will be very close to θ_2 , but C_0 will decrease as the plume spreads and meanders. By mass conservation, if the mean plume width is $L(X)$, with $L(0) = L_0$, then we expect $C_0 = \theta_1(L_0/L)^j$, where j is 1 for a line source, 2 for a point source and 3 for an instantaneous release. For the line source this gives

$$\frac{\theta_{\max}}{C_0} \approx \frac{\theta_2 L(X)}{\theta_1 L_0}. \tag{2.7}$$

So close to the source we expect θ_{\max}/C_0 to increase downstream.

Further downstream we expect (2.7) to provide an upper bound for θ_{\max}/C_0 , since diffusion reduces θ_{\max} while hardly affecting C_0 . Consider a case when there is an upper limit l on the length scale of the turbulence, and the fluid is unbounded. (Such a flow could be approximated, for example, by grid turbulence in a wind tunnel whose

dimensions are much larger than the mesh length of the grid.) Very far downstream, eventually the plume width is much greater than l and a state is reached where the centreline is so far from ambient (i.e. zero concentration) fluid that, before such fluid can be entrained all the way to the centreline, diffusion will have brought its concentration into equilibrium with that in the surrounding parts of the plume. This will be the case if the time taken to diffuse a distance l is much less than the time taken to advect ambient fluid to the centreline, i.e. L/l is much larger than the Péclet number, which will be the case far enough downstream. So we expect that the concentration p.d.f. on the centreline will tend to $\delta(C_0)$, and θ_{\max} will tend to the local mean concentration, i.e. $\theta_{\max}/C_0 \rightarrow 1$. In experiments we are unlikely to approach this ultimate state, but this argument does suggest that as one goes downstream θ_{\max}/C_0 increases away from the source, reaches a maximum and then decreases towards 1.

Variations of θ_{\max} result from variations in the amount by which molecular diffusion reduces concentrations. In the cross-stream direction we expect that, far enough from the centreline, θ_{\max} will tend to zero, since any source fluid arriving far out will have taken a long time to get there, during which diffusion reduces the concentrations virtually to zero. C also decreases away from the centreline, mainly because of the increasing rarity of sheets and strands containing high concentrations, an effect associated with the relatively fast-acting turbulent advection. Diffusion acts on a much slower time scale, so we expect θ_{\max} to decrease more slowly away from the centreline than does C , i.e. θ_{\max} will decrease on a scale much larger than L . (In the limiting case of zero molecular diffusion the concentration always remains at its source value. In this case θ_{\max} is uniform in space, and equal to the maximum source concentration, while the mean concentration decreases away from the centreline, because of turbulent advection.) Thus we expect that $\theta_{\max}/C \rightarrow \infty$ as $C/C_0 \rightarrow 0$, with $\theta_{\max}/C_0 \rightarrow 0$. In practice we can only make reasonable measurements of the moments out to $|Z|/L \sim 2$, and over this range we expect θ_{\max} to be almost constant. This picture is consistent with the time series of concentration shown in figure 1 of Mylne & Mason (1991). That figure shows the typical spiky nature of concentration traces. The largest concentration at the centreline position is a little more than $3C$, and at the position away from the centreline it is of order $30C$. At a fixed off-centreline distance, far downstream the argument used above for the centreline still applies (but the further from the centreline, the further downstream one has to go before the asymptotic result is approached), so we expect that

$$\frac{\theta_{\max}}{C_0} \longrightarrow \frac{C}{C_0} \quad \text{as } X \rightarrow \infty.$$

Far downstream, since we expect the p.d.f. to approach a delta function, we expect k to become large, with the GPD having the type of shape illustrated in figure 1(c). For a uniform source, on the centreline this will also be true close to the source. So we might expect that on the centreline k has a minimum at some downstream distance. Far from the centreline we expect the highest concentrations to occur only rarely, suggesting the shape in figure 1(a), and thus $k < 0.5$. As with θ_{\max} , we expect k to vary more slowly than C in the cross-stream direction, since it is determined by the distribution of high concentrations and so is controlled by molecular diffusion.

2.4. The observed spatial variation of the GPD parameters

Figure 6(a) shows the observed variation with downstream distance of the centreline values of k , a/C_0 and θ_{\max}/C_0 , estimated from the data of Sawford & Tivendale (1992). As expected, θ_{\max}/C_0 increases away from the source, to a maximum of about

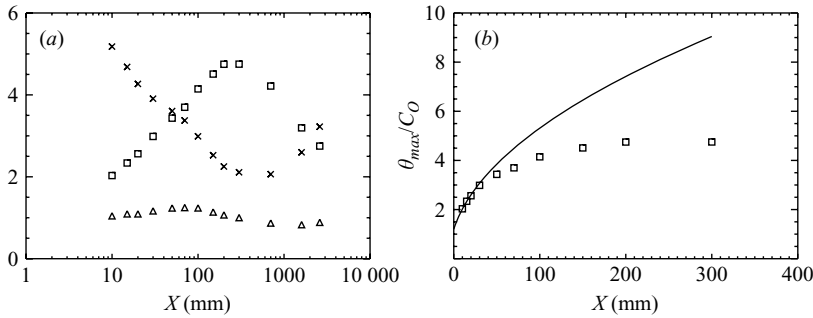


FIGURE 6. Variation on the centreline of GPD parameters (estimated from the data of Sawford & Tivendale 1992) with downstream distance X . (a) θ_{\max}/C_0 (squares), a/C_0 (triangles) and $10k$ (crosses), (b) θ_{\max}/C_0 (squares), and the approximation to θ_{\max}/C_0 in the no diffusion case based on (2.8) (curve).

4.75 at a downstream distance of about 250 mm, before decreasing to about 2.75 at the furthest distance of 2600 mm. Figure 6(a) also confirms that, as expected, k decreases to a minimum, before increasing further downstream. In figure 6(b) we compare the relatively near-source behaviour of θ_{\max}/C_0 with an estimate of the behaviour in the absence of molecular diffusion. In the no diffusion case we use (2.7), and assume that (following the classical large-time fluid particle analysis of Batchelor 1949)

$$\frac{L(X)}{L_0} = \sqrt{1 + \gamma X}, \tag{2.8}$$

where γ is a constant, i.e. a form which satisfies $L(0) = L_0$ and is consistent with the expected square root dependence on X far downstream. The parameters in this form were determined by fitting to the measured values of θ_{\max}/C_0 at 10 mm and 15 mm (on the assumption that diffusion will have had relatively little effect there), giving $\theta_2/\theta_1 \approx 1.20$. (Note that if (2.8) is replaced with a near-source behaviour with X replaced by X^2 , then the estimated value of θ_2/θ_1 becomes 1.75.) As expected, this estimate is progressively larger than the measured values of θ_{\max}/C_0 , showing the cumulative effect of molecular diffusion.

Figure 6(a) shows that a/C_0 varies relatively little, with values quite close to 1 for all downstream distances. This implies that θ_{\max}/C_0 and k are roughly inversely proportional, as seen in the figure.

Figure 7 shows the variation of the parameters across the plume. There is no clear pattern to the variation of θ_{\max} , although most of the values are a little larger than on the centreline. However, on physical grounds there is no reason to believe that the maximum concentration would increase away from the centreline. The values seen here probably just reflect the inevitable uncertainty in the estimates. This uncertainty would be expected to increase away from the centreline, and also as one goes downstream, which is consistent with the observed scatter in these results. It may also be that any underestimation of θ_{\max} is greater on the centreline. The conclusion we draw is that θ_{\max} is roughly constant across the plume, at least as far out as reasonable measurements can be made, consistent with the arguments advanced above. The values of θ_{\max}/C at the smallest values of C/C_0 shown in figure 7(a) are an order of magnitude larger than the values of θ_{\max}/C on the centreline, consistent with our argument above that $\theta_{\max}/C \rightarrow \infty$ in the periphery.

Munro *et al.* (2003a) analysed data from a point source field experiment, in the relative frame of reference. They found that θ_{\max} decreased to about 25% of its

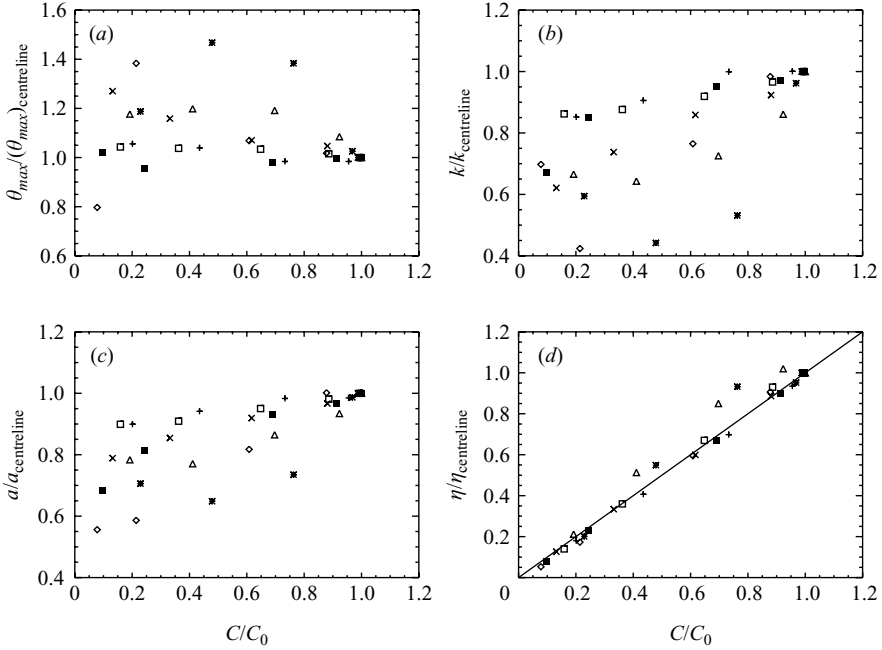


FIGURE 7. Variation across the plume of GPD parameters normalized by their centreline values. (a) θ_{\max}' , (b) k , (c) a , (d) η . Values are shown at a selection of downstream distances: 10 mm (■), 30 mm (□), 100 mm (×), 150 mm (+), 300 mm (△), 1600 mm (*), 2600 mm (◇). The line in (d) is that on which the normalized value of η equals C/C_0 .

centreline value by distances of $3L$ – $4L$ from the centreline (see figure 4 of Munro, Chatwin & Mole 2003*b* for the cross-plume variation of C). The measurements in that experiment were made by a Lidar, with a spatial resolution of about 1.4 m. The thin sheets and strands containing the largest concentrations would not be resolved in this case, with a consequent reduction in the highest measured concentrations. Further from the centreline the sheets and strands are more sparsely distributed (the main cause of the decrease of C), and the lack of resolution would cause larger reductions in measured high concentrations. We believe this explains most of the cross-plume variation of θ_{\max}' found by Munro *et al.* (2003*a*).

In the experiments analysed here, the spatial resolution is limited by the cold wire length of 0.4 mm, which is comparable to the conduction cutoff length λ_c . (Temporal resolution is much better than λ_c/U and so should be less of a problem.) So we expect that there will be some smoothing of the very smallest scales in the concentration field. Highest concentrations would be reduced most so, as well as reducing θ_{\max}' , smoothing would probably increase k and decrease a . It would also reduce β but, because of the normalization of moments, the effect on other parameters used in our modelling, like α and a_n , is unclear but probably small.

From figure 7, k and a both appear to decrease away from the centreline, but the magnitude of the decrease is fairly small, as expected, except at the further downstream positions where the uncertainty is likely to be larger. The larger decrease further downstream might also be a reflection of the relatively faster action of diffusion once the scalar is found in thin sheets and strands: see the arguments in the Appendix.

η decreases away from the centreline. If we denote the centreline value of η by η_0 , then η/η_0 is close to being equal to C/C_0 . If (2.4) held for $n=1$, so even the mean concentration $m_1 (= C)$ were dominated by the GPD tail, then we would have $C \approx \eta a/(1+k)$. Since we do not expect a and k to vary much across the plume, and since they both appear to decrease away from the centreline, we would then expect that η/C would be fairly constant across the plume, giving $\eta/\eta_0 \approx C/C_0$.

3. Deriving properties of high concentrations from the moment model

3.1. The relationship between the parameters describing the moments

The expressions for the central moments, (1.6), can be used to calculate the absolute moments m_n , defined by (2.3). Letting

$$M_n = \frac{m_n}{\hat{C}(\alpha\beta C_0)^n}, \quad B = \frac{1}{\beta}, \quad D = \left(\frac{1}{\beta} - 1\right) \hat{C},$$

we obtain

$$\left. \begin{aligned} M_2 &= 1 + (B + 1)D, \\ M_3 &= \lambda_3^2 + 3D + (B + 2)D^2, \\ M_4 &= \lambda_4^3 + 4\lambda_3^2 D + 6D^2 + (B + 3)D^3, \\ M_5 &= \lambda_5^4 + 5\lambda_4^3 D + 10\lambda_3^2 D^2 + 10D^3 + (B + 4)D^4, \\ &\vdots \end{aligned} \right\} \quad (3.1)$$

We now consider the behaviour of the n th moment, at a fixed downstream distance, as we go far from the centreline. We then have $D \ll 1$, so

$$M_n \approx \lambda_n^{n-1}. \quad (3.2)$$

Now,

$$\mu_n = m_n - nCm_{n-1} + \frac{1}{2}n(n-1)C^2m_{n-2} + \dots + \frac{1}{2}n(n-1)(-C)^{n-2}m_2 - (n-1)(-C)^n.$$

By (2.4) and (2.5) we have

$$\frac{m_n}{nCm_{n-1}} \approx \frac{a}{C(1+nk)} = \frac{\theta_{\max}}{C(n+1/k)}.$$

If we assume that k does not tend to zero far from the centreline, which seems consistent with figure 7(b), then, since $\theta_{\max}/C \rightarrow \infty$, we also have $m_n/(nCm_{n-1}) \rightarrow \infty$ far from the centreline. So we then have

$$\mu_n \approx m_n, \quad (3.3)$$

giving

$$K_n \approx \frac{\lambda_n^{n-1}}{\hat{C}^{n/2-1}} \gg 1.$$

Equation (1.5) shows that

$$K_n \approx a_n K_3^{n-2},$$

and combining these two results we have

$$\lambda_n^{n-1} \approx a_n \lambda_3^{2(n-2)}. \quad (3.4)$$

This result was derived previously by Schopflocher *et al.* (2007). Since we expect λ_n and a_n to be approximately constant across the plume, (3.4) applies everywhere, even though it is derived by considering the plume periphery. So the moments can be characterized in terms of α , β , λ_3 and the a_n . An advantage of using a_n rather than λ_n is that the a_n can be determined more easily from measurements at just a few points.

Combining (3.1) and (3.4) gives

$$\left. \begin{aligned}
 M_2 &= 1 + (B + 1)D, \\
 M_3 &= \lambda_3^2 + 3D + (B + 2)D^2, \\
 M_4 &= a_4\lambda_3^4 + 4\lambda_3^2D + 6D^2 + (B + 3)D^3, \\
 M_5 &= a_5\lambda_3^6 + 5a_4\lambda_3^4D + 10\lambda_3^2D^2 + 10D^3 + (B + 4)D^4, \\
 M_6 &= a_6\lambda_3^8 + 6a_5\lambda_3^6D + 15a_4\lambda_3^4D^2 + 20\lambda_3^2D^3 + 15D^4 + (B + 5)D^5, \\
 &\vdots \\
 M_n &= a_n\lambda_3^{2(n-2)} + na_{n-1}\lambda_3^{2(n-3)}D + \frac{1}{2}n(n-1)a_{n-2}\lambda_3^{2(n-4)}D^2, \\
 &\quad + \dots + \frac{1}{2}n(n-1)D^{n-2} + (B + n - 1)D^{n-1}, \\
 &\vdots
 \end{aligned} \right\} \tag{3.5}$$

3.2. Reduction of the number of parameters

We now show that, by considering the behaviour far from the centreline, we can reduce the number of parameters needed to describe the moment structure to just five, namely α , β , λ_3 , a_4 and a_5 .

By the definition of M_n we have

$$\frac{m_{n-1}}{m_n} = \frac{M_{n-1}}{\alpha\beta C_0 M_n}.$$

We can then write (2.6) as

$$\frac{M_{n-1}}{M_n} \approx \frac{1}{a'} \left(\frac{1}{n} \right) + \frac{k}{a'}, \tag{3.6}$$

where

$$a' = \frac{a}{\alpha\beta C_0}.$$

Using (3.5) then allows us to model the distribution of high concentrations in terms of the parameters α , β , λ_3 and a_n which describe the moment structure.

As before, we can make progress by considering the plume periphery, where $D \rightarrow 0$. We then have

$$M_n \approx a_n\lambda_3^{2(n-2)} + na_{n-1}\lambda_3^{2(n-3)}D,$$

giving

$$\frac{M_{n-1}}{M_n} \approx \frac{a_{n-1}}{\lambda_3^2 a_n} \left\{ 1 + \left[\frac{(n-1)a_{n-2}}{a_{n-1}} - \frac{na_{n-1}}{a_n} \right] \frac{D}{\lambda_3^2} \right\}. \tag{3.7}$$

First, we consider only the leading-order term on the right-hand side. Given the behaviour of the measured moments discussed in §2.2 (and analysis of the Lidar data used in Munro *et al.* 2003*a, b* also gives a good linear fit down to $n = 4$: R. J. Munro, personal communication) it seems reasonable to assume that (3.6) holds down to $n = 4$. Then we can use the ratios for $n = 4$ and $n = 5$ (with $a_3 \equiv 1$) to determine

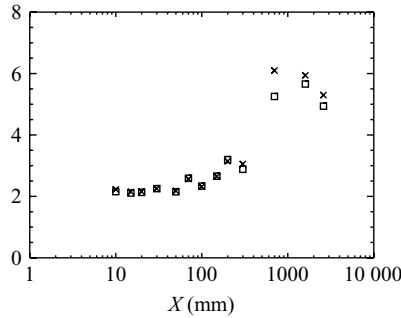


FIGURE 8. Variation with downstream distance X of a_6 (squares), and of the expression given by (3.11) (crosses).

k and a' :

$$k \approx \frac{5a_4^2 - 4a_5}{20(a_5 - a_4^2)} \tag{3.8}$$

and

$$a' \approx \frac{\lambda_3^2 a_4 a_5}{20(a_5 - a_4^2)}. \tag{3.9}$$

Since we also expect (3.6) to hold for $n = 6, 7, \dots$ this implies that a_6, a_7, \dots can all be expressed in terms of a_4 and a_5 . We find that

$$\frac{a_n}{a_{n-1}} = \frac{na_4 a_5}{(5n - 20)a_4^2 - (4n - 20)a_5} \quad \text{for } n = 6, 7, \dots \tag{3.10}$$

In particular, this gives

$$a_6 = \frac{3a_4 a_5^2}{5a_4^2 - 2a_5}. \tag{3.11}$$

Figure 8 compares the measured a_6 with (3.11), using the values of a_4, a_5 and a_6 determined by Schopflocher *et al.* (2007). The agreement is very good. Thus, by considering high concentrations far from the centreline, we have shown that the set of parameters describing the moment structure can be reduced to only five: $\alpha, \beta, \lambda_3, a_4$ and a_5 .

3.3. A model for the maximum concentration

We can rewrite (3.10) as

$$\frac{a_{n-1}}{a_n} = \frac{1}{r} \left\{ 1 - \frac{20}{n} \left(\frac{a_4^2 - a_5}{5a_4^2 - 4a_5} \right) \right\}, \tag{3.12}$$

where

$$r = \frac{a_4 a_5}{5a_4^2 - 4a_5}. \tag{3.13}$$

We then obtain

$$\frac{(n - 1)a_{n-2}}{a_{n-1}} - \frac{na_{n-1}}{a_n} = -\frac{1}{r},$$

so (3.7) becomes

$$\frac{M_{n-1}}{M_n} \approx \frac{1}{\lambda_3^2 r} \left\{ 1 - \frac{20}{n} \left(\frac{a_4^2 - a_5}{5a_4^2 - 4a_5} \right) \right\} \left(1 - \frac{D}{\lambda_3^2 r} \right). \tag{3.14}$$

Comparing (3.6) and (3.14) we find that k satisfies (3.8) even when we include the next order term. Since it is this next order term, containing D , which first introduces cross-stream variations, this suggests that we might expect k to be approximately constant across the plume. In fact, the full calculation, as discussed below, shows that k decreases slightly away from the centreline, as found in figure 7(b) for the measured values.

Comparing (3.6) and (3.14) also allows us to determine $\theta_{\max}/C_0 = \alpha\beta a'/k$:

$$\frac{\theta_{\max}}{C_0} \approx \frac{\alpha\beta\lambda_3^2 a_4 a_5}{5a_4^2 - 4a_5} + (1 - \beta) \frac{C}{C_0}. \quad (3.15)$$

Note that the only place where the large n approximation has been used in this derivation is in obtaining (3.6). The total cross-plume variation of θ_{\max}/C_0 given by (3.15) is $1 - \beta$, with the largest value on the centreline. For the Sawford & Tivendale (1992) data the measured values of β are all between 0.62 and 0.85, so this variation is small.

The physical arguments in §2.3 suggested that far enough from the centreline θ_{\max}/C_0 would tend to zero. This is consistent with (3.15), since, at the off-centreline distances where diffusion has had time to reduce θ_{\max}/C_0 significantly, we also expect diffusion to have reduced β significantly. Far downstream the total time for diffusion to occur also increases, and eventually we expect $\beta \rightarrow 0$, even on the centreline. Equation (3.15) then suggests that

$$\frac{\theta_{\max}}{\theta_0} \rightarrow \frac{C}{C_0},$$

in exact agreement with the limit predicted by the physical arguments in §2.3.

The asymptotic expression (3.7), used to derive (3.15), is strictly only valid in the plume periphery. As we go towards the centreline, C/C_0 no longer gives a small correction in general, so (3.15) will not necessarily give the correct asymptotic result. Nevertheless, we might hope that it still gives a reasonable first guess for θ_{\max}/C_0 . If we want to find the model predictions for k and θ_{\max}/C_0 without assuming small C/C_0 , and hence small D , then we need to calculate the moment ratios using the full expressions in (3.5), together with (3.10). Figure 9 shows some linear fits obtained in this way. As with figure 2, we find a good fit down to $n = 4$.

In figure 10 we compare the resulting variation of k with that predicted by the asymptotic result (3.8). The asymptotic result is very accurate, except near the centreline relatively close to the source. The full result shows that k decreases slightly away from the centreline, as found for the measured values in figure 7(b).

Figure 11 compares the full and asymptotic results for θ_{\max}/C_0 . The difference between these results is very small, and much less than the expected uncertainty in the direct experimental estimates of θ_{\max}/C_0 . Except for a small range of C/C_0 values at $X = 300$ mm, (3.15) slightly overestimates θ_{\max}/C_0 . We can use the asymptotic result (3.15) as our model prediction for θ_{\max}/C_0 without any real loss.

3.4. Comparison of model predictions with experimental data

Figure 12 compares the downstream variation of the model predictions (using the measured values of α , β , λ_3 , a_4 and a_5) for θ_{\max}/C_0 , k and a/C_0 with that for the experimentally estimated values in figure 6. The model predictions for θ_{\max}/C_0 increase downstream, but are larger than the estimates. Beyond $X = 300$ mm they become unreliable, with negative or very large values. (We note that as we go downstream, and particularly beyond 300 mm, the variation in values of α , β and λ_3 between repeat measurements increases significantly; we have used averaged values.)

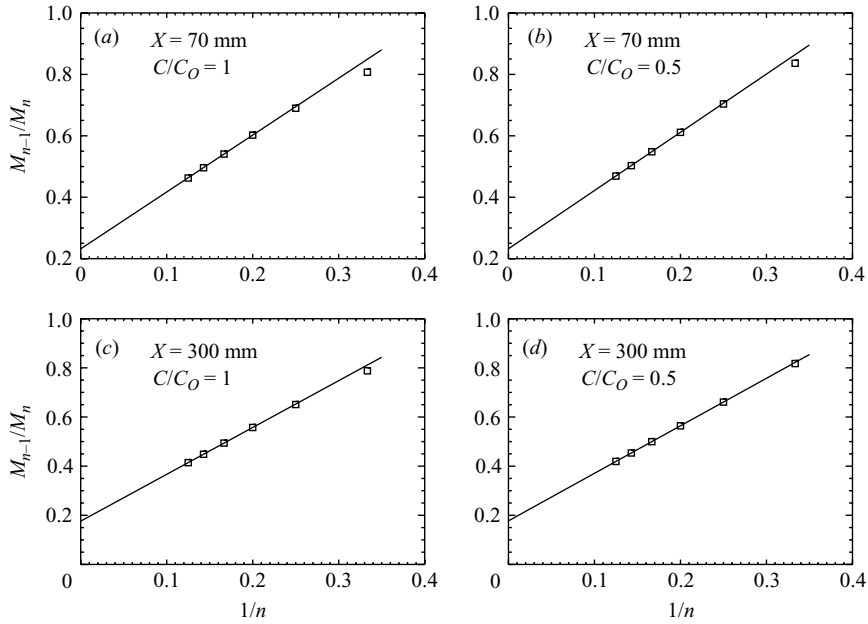


FIGURE 9. Linear fits to the moment ratios calculated from (3.5) and (3.10).

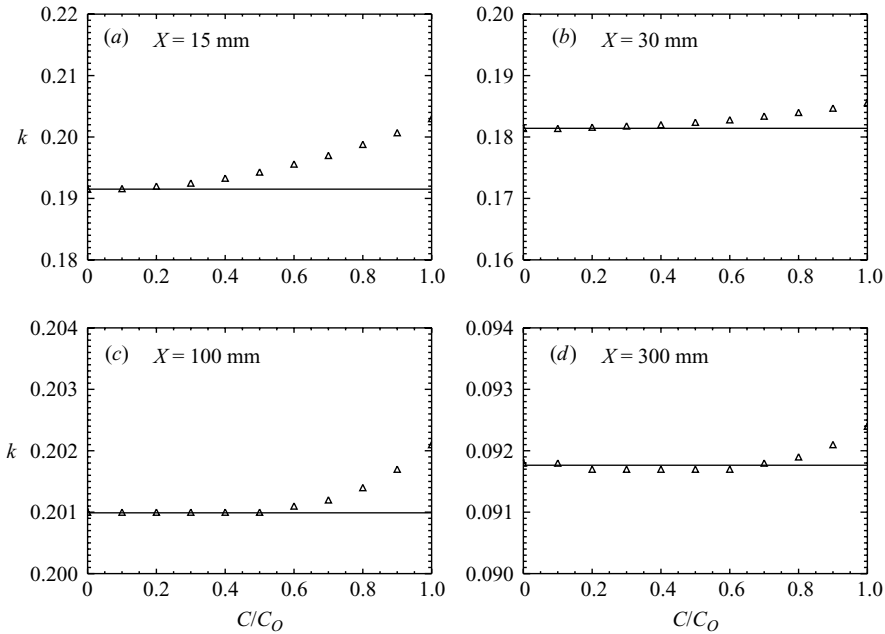


FIGURE 10. k calculated from (3.5) and (3.10) (triangles), and calculated from (3.8) (line).

The predictions for k tend to decrease, but are too small, and at large X they become close to zero rather than increasing again. The very small values of the predicted k at large X mean that small uncertainties in k will lead to large uncertainties in θ_{\max}/C_0 . The predicted values of a/C_0 follow the same trends as the estimated values, but are roughly a factor of 2 smaller.

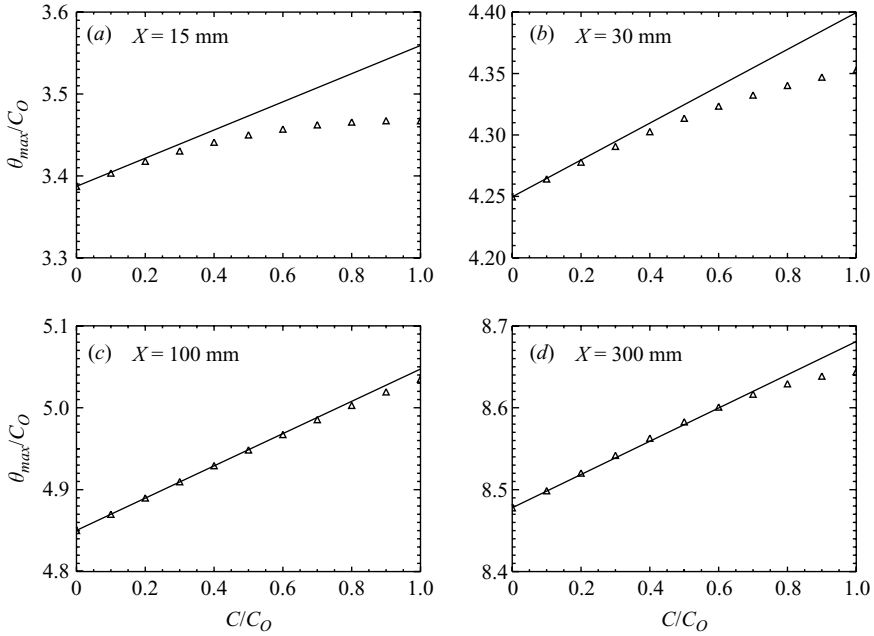


FIGURE 11. θ_{\max}/C_0 calculated from (3.5) and (3.10) (triangles), and calculated from (3.15) (line).

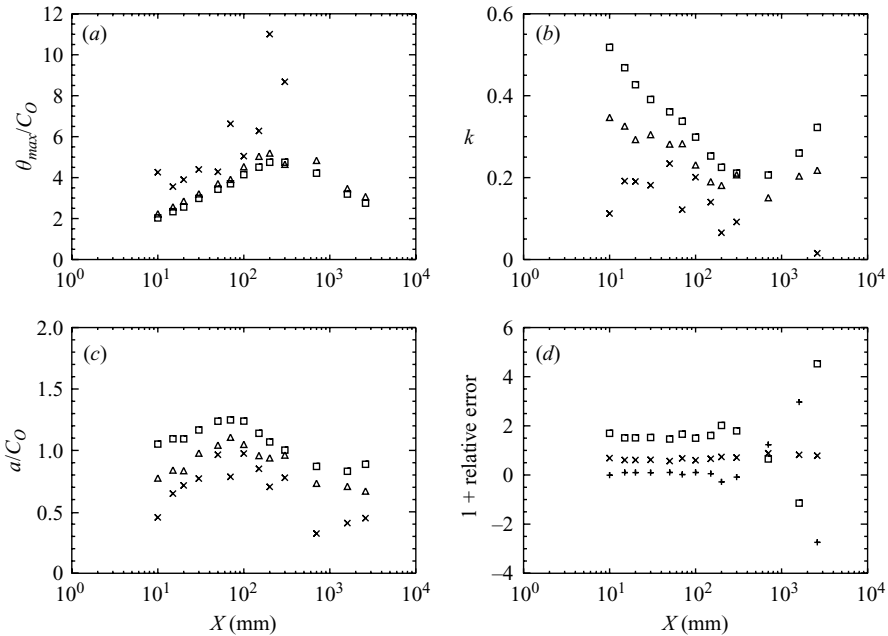


FIGURE 12. (a), (b) and (c) give the comparison on the centreline between model values calculated from (3.8), (3.9) and (3.15) (crosses), values calculated directly from the measurements by least-squares fits (squares), and values calculated directly from the measurements by a linear fit to the moment ratios for $n = 7$ and $n = 8$ (triangles): (a) θ_{\max}/C_0 , (b) k , (c) a/C_0 . In (d) we show the errors estimated from (3.8), (3.9) and (3.15) under the assumption that there is a 5% relative error in a_5 (squares θ_{\max}/C_0 , plus signs k , crosses a/C_0).

It is always difficult to make precise estimates of properties, like those shown in figure 12, of the high concentration tail of the p.d.f. To give a further indication of the possible level of uncertainty we calculated the errors in θ_{\max}/C_0 , k and a/C_0 (estimated from (3.8), (3.9) and (3.15)) which would result from errors in a_5 . Figure 12(d) shows the results for a relative error in a_5 of 5%, using the estimated values of a_4 and a_5 at each downstream distance. At most distances this results in the estimate of θ_{\max}/C_0 being nearly two times too large, and at large X the errors become very variable. This is broadly consistent with what we see in figure 12(a–c). Given the possible level of uncertainty, the agreement in figure 12(a–c) is fairly reasonable.

We note that although the parameter values used in calculating the model predictions are derived from the same data set as the estimates of θ_{\max}/C_0 , they are derived in a rather different manner. The estimates use the concentration moments at one point in space to give θ_{\max}/C_0 at that point. On the other hand, at each downstream distance, α , β and λ_3 are estimated from the relationship between the 2nd and 3rd moments and C in the plume cross-section; a_4 and a_5 are estimated from the relationship between the normalized 4th and 5th moments and the skewness, in the plume cross-section. So there is no direct connection between the model predictions and the estimates of θ_{\max}/C_0 that were compared, other than those which reflect an underlying physical structure.

In addition to the uncertainty discussed above, a possible partial explanation of the differences between the model predictions and the estimated values shown in figure 12 can be provided by the argument given at the end of §2.2. If the gradient of the linear fits to the moment ratios is underestimated then the result is that θ_{\max} is underestimated and a is overestimated. Therefore, k will be overestimated by a combination of both these factors. To test this argument, in figure 12(a–c) we also show the values calculated from a linear fit to the moment ratios for $n=7$ and $n=8$. These give a significantly better agreement for k and a/C_0 , and a slightly better agreement for θ_{\max}/C_0 , but they are more noisy. If we used a similar linear fit for larger n we might expect even better agreement, but at the expense of greater noise. Even given this improved agreement, it still seems that the model predictions of θ_{\max}/C_0 might well be greater than the direct estimates, so the model would give a conservative estimate of the maximum concentration.

4. Discussion

4.1. General discussion and conclusions

Arguments based on the small-scale physics of turbulent dispersion suggest that the high-concentration tail of the p.d.f. of concentration ought to have a universal character. The abstract arguments of statistical extreme value theory suggest that the high-concentration tail ought to be well approximated by a Generalized Pareto Distribution. Together, these provide a compelling argument for universal high-concentration GPD tails. This is borne out by direct fits to measured concentrations in a variety of experiments, both in the field and the wind tunnel (Lewis & Chatwin 1995b; Mole *et al.* 1995; Anderson *et al.* 1997; Munro *et al.* 2001; Schopfloch 2001; Schopfloch & Sullivan 2002). A number of methods have been used to fit GPD tails to experimental data, and it is possible to construct statistical models based on these fits. However, these methods do not easily lend themselves to physical modelling of the high concentrations.

Direct numerical simulation (DNS) would, in principle, be able to predict the high-concentration tails, but modelling the tails would place even larger demands

on computing power than in more common applications of DNS. Using large eddy simulation (LES) would reduce the demands on computing power, but the parametrized small scales are those on which the largest concentrations are found, although Xie *et al.* (2007) had reasonable success using LES to model the maximum concentration from point sources in a boundary layer. It is not clear that the kind of p.d.f. methods described, for example, in §12.7.4 of Pope (2000) will perform well in the high-concentration tails. Most other physical modelling approaches are based on concentration moments, so a method of connecting moments to the high-concentration tails would be a great advantage.

In §2.2 we derived such a method. We found an approximate linear relationship between the ratios of successive moments, and the reciprocal of the moment order. We found that this relationship, given by (2.6), gave an excellent fit to the measured moment ratios. The parameters of the GPD tail are determined by this linear fit. Thus, using this method, any model which predicts a sufficiently large number of moments would be able to predict the behaviour at high concentrations. In particular, it would allow the prediction of the maximum possible concentration θ_{\max} . We analysed the measurements of Sawford & Tivendale (1992), for a steady line source in wind tunnel grid turbulence. If the results that we obtained for the moment ratios, shown in figures 2 and 9, are typical, then reasonable estimates can probably be obtained from the first 5 or 6 moments.

Using the relationships between moments proposed by Chatwin & Sullivan (1990a), Sawford & Sullivan (1995) and Mole & Clarke (1995), we derived an analytical expression (3.15) for θ_{\max}/C_0 , where C_0 is the centreline mean concentration. This expression depends on the parameters α , β , λ_3 , a_4 and a_5 , and (weakly) on C/C_0 , where C is the local mean concentration. The comparison, in §3.4, between this model expression and θ_{\max}/C_0 estimated directly from (2.6) shows promise, suggesting that the model gives a good first guess for θ_{\max}/C_0 . In the next section we discuss possible methods for modelling the parameters.

4.2. Modelling of the parameters

To model θ_{\max} , independently of any particular experimental measurements, we then need models for the parameters α , β , λ_3 , a_4 and a_5 , and for C/C_0 . Since models for C are the subject of an extensive literature (see e.g. Anand & Pope 1985 for a model for C for a line source in grid turbulence), and since in our models θ_{\max}/C_0 depends only weakly on C/C_0 , we shall only deal with possible approaches to modelling the parameters.

Since α , β , λ_3 , a_4 and a_5 are determined by relationships between the first 5 concentration moments, any model for the spatial variation of these moments would, in principle, also yield these parameters. Here we shall consider approaches based on our own moment models, referred to above.

Clarke & Mole (1995), Labropulu & Sullivan (1995) and Mole (1995, 2001) considered ways to model α and β (in effect λ_3 was taken to be 1). These were all based on integrating moments over ‘all space’ (which in the present context means throughout the plume cross-section), and making a closure assumption for $E \{ \Gamma^{n-2} (\nabla \Gamma)^2 \}$ in terms of the moments, where Γ is the concentration. These models have been shown to give qualitative agreement with observation, although it remains to carry out a thorough quantitative assessment against measurements. For modelling α and β , the evolution equations for the 2nd and 3rd moments were used. For a steady line source, in these models far downstream α tends to a constant (≈ 1.182 in Mole 2001, and an indeterminate, but probably order 1, constant in Labropulu &

Sullivan 1995) and $\beta \rightarrow 0$, with $\beta \propto X^{-1/2}$. We note that these models all assume that β is constant throughout the plume cross-section, whereas we expect that very far from the centreline β will tend to zero. So these models ought to be relevant to the range over which reliable measurements can be made, but not beyond that.

When the $\lambda_n (\neq 1)$ are included, the same approach could still be used, but the equations for the fourth to sixth moments would also need to be used. Then λ_4, λ_5 and λ_6 would be replaced using (3.4), and a_6 would be replaced using (3.11). This would then give a set of five equations for the five unknowns. If we could derive independent expressions for a_4 and a_5 then the number of simultaneous differential equations needing to be solved would be reduced, and we consider one such possibility below.

We assume that far from the centreline η becomes small. This is supported by figure 7(d). Far from the centreline, from (1.3), (2.4), (2.5) and (3.3) we have

$$\sigma^n K_n \approx \frac{\eta n! a^n}{(1+k)(1+2k)\cdots(1+nk)}, \tag{4.1}$$

where $\sigma = (\mu_2)^{1/2}$ is the standard deviation of concentration. In particular, we have

$$\begin{aligned} \sigma^2 &\approx \frac{2\eta a^2}{(1+k)(1+2k)}, \\ \sigma^3 K_3 &\approx \frac{6\eta a^3}{(1+k)(1+2k)(1+3k)}. \end{aligned}$$

The approach of Mole & Clarke (1995) gives

$$\sigma^{2(n-3)}(\sigma^n K_n) = a_n(\sigma^3 K_3)^{n-2} + b_n\sigma^6(\sigma^3 K_3)^{n-4} + \dots$$

To leading order in the small parameter η we determine a_n (the next order determines b_n , and so on):

$$a_n = \frac{n!(1+3k)^{n-3}}{2 \times 3^{n-2}(1+4k)(1+5k)\cdots(1+nk)}. \tag{4.2}$$

This is essentially an extension of the result given in equation (A.5) of Lewis *et al.* (1997). In particular, (4.2) gives

$$a_3 = 1, \quad a_4 = \frac{4(1+3k)}{3(1+4k)}, \quad a_5 = \frac{20(1+3k)^2}{9(1+4k)(1+5k)}.$$

For $k > 0$ these give $1 < a_4 < 4/3$ and $1 < a_5 < 20/9$. Most experimentally determined values of a_4 and a_5 fall within these ranges.

In figure 13(a) we show the resulting values of a_4 and a_5 , calculated using estimated peripheral values of k . We estimated these very roughly, by taking the measurements of k closest to and furthest from the centreline, and linearly extrapolating to $C/C_0 = 0$. Also plotted are the directly measured values of a_4 and a_5 . The agreement is reasonable, except at the furthest downstream positions, but the measured values are slightly larger. If we invert the above relationships, we can use the measured values of a_4 and a_5 to estimate the peripheral k . These modelled values of k are plotted in figure 13(b), together with the measured centreline values of k . The modelled values obtained from a_4 and from a_5 agree with each other fairly well. If we ignore the furthest downstream positions, where variability in measured parameters is significant and some of the modelled k values become negative, then the modelled peripheral k values are about 40–70% of the measured centreline values, with this

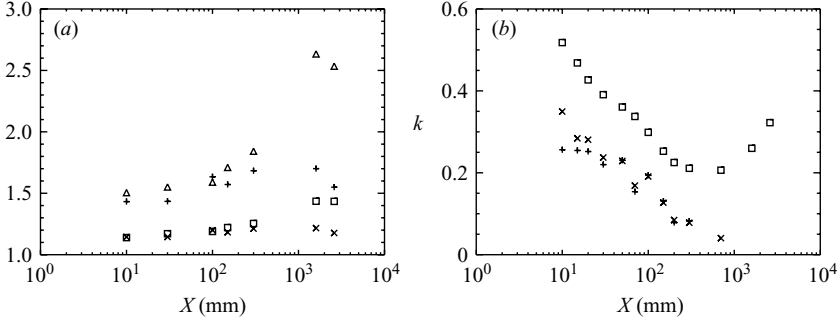


FIGURE 13. (a) Measured a_4 (\square), modelled a_4 (\times), measured a_5 (\triangle) and modelled a_5 ($+$), (b) Measured centreline k (\square) and modelled peripheral k using a_4 (\times) and a_5 ($+$).

proportion decreasing downstream, in rough agreement with what one would expect from figure 7(b). These results seem to provide support for the model relating a_4 and a_5 to k .

Combining the expressions for a_4 and a_5 we have

$$a_5 = \frac{5a_4^2}{8 - 3a_4}.$$

So we can treat a_5 as being determined by either k or a_4 , thus reducing by one the number of parameters needing to be modelled. We note also that (4.2) gives

$$\frac{a_n}{a_{n-1}} = \frac{n(1 + 3k)}{3(1 + nk)} = \frac{na_4a_5}{5(n - 4)a_4^2 - 4(n - 5)a_5}, \tag{4.3}$$

in agreement with (3.10). Since

$$\frac{n(1 + 3k)}{3(1 + nk)} = 1 + \frac{n - 3}{3(1 + nk)},$$

(4.3) shows that the a_n form a monotonically increasing sequence, with $a_n \rightarrow \infty$ as $n \rightarrow \infty$.

If we now substitute for a_4 and a_5 in (3.15), we obtain

$$\frac{\theta_{\max}}{C_0} \approx \alpha\beta\lambda_3^2 \left(1 + \frac{1}{3k} \right) + (1 - \beta)\frac{C}{C_0}. \tag{4.4}$$

Equation (4.2) was derived by considering the plume periphery. The a_n are constant across the plume, but k may vary, so the value of k in (4.4) is that appropriate to the periphery. Far downstream we expect that α and λ_3 will tend to constants, and that $k \rightarrow \infty$ and $\beta \rightarrow 0$. From (4.2) we then expect that $a_n \rightarrow 1$, and (4.4) becomes

$$\frac{\theta_{\max}}{C_0} \sim \alpha\beta\lambda_3^2 + \frac{C}{C_0}.$$

We wish to thank Philip Chatwin for his invaluable contributions over many years. NM visited PJS under a Royal Society International Outgoing Short Visit grant, and PJS received financial support from the National Science and Engineering Research Council of Canada. We are particularly grateful to Brian Sawford and Charles Tivendale for making their data available to us.

Appendix. Thoughts on the Pe and Re dependence of θ_{\max}/C_0

We let u and l be the velocity and length scales for turbulent velocity fluctuations, with Péclet number $Pe = ul/\kappa$ and Reynolds number $Re = ul/\nu$. We also let L be the mean plume width (i.e. the width of the profile of mean concentration C), $L = L_0$ at the source, T_A be an advection time scale for the reduction of C_0 , T_D be a diffusion time scale for the reduction of θ_{\max} , and $\lambda_C = (\nu\kappa^2/\epsilon)^{1/4}$ be the conduction cutoff length.

A.1. *Relative time scales and the spatial variation of θ_{\max}/C_0*

A.1.1. *Downstream variations*

If $\lambda_C \lesssim L_0$ then near the source we expect the relevant length scale for both the spreading of the mean plume (and, hence, the reduction of C_0) and the reduction of θ_{\max} by diffusion to be the mean plume width L . Thus

$$T_A = \frac{L}{u} \quad \text{and} \quad T_D = \frac{L^2}{\kappa},$$

so

$$\frac{T_D}{T_A} = \frac{uL}{\kappa} = \left(\frac{L}{l}\right) Pe.$$

Pe is large, and near the source L/l will usually be small. In the Sawford & Tivendale (1992) experiments $l/L_0 \sim 100$ and Re based on mean velocity is 8500. If we assume that the Schmidt number is of order 1, and u is an order of magnitude smaller than the mean velocity, then Pe is of order 1000 and

$$\frac{T_D}{T_A} \sim 10.$$

In this regime the reduction of θ_{\max} proceeds more slowly than the reduction of C_0 , so as we go away from the source θ_{\max}/C_0 increases.

Once we are far enough downstream for the mean plume to be wider than the turbulence length scale, i.e. $l \lesssim L$, then, if we assume that concentration is now found largely in sheets and strands of thickness close to the conduction cutoff,

$$T_A = \frac{l}{u} \quad \text{and} \quad T_D = \frac{\lambda_C^2}{\kappa} = \left(\frac{\nu}{\epsilon}\right)^{1/2},$$

so

$$\frac{T_D}{T_A} = Re^{-1/2} \left(\frac{u^3}{\epsilon l}\right)^{1/2} \sim Re^{-1/2} \ll 1.$$

So in this regime we expect that θ_{\max} is reduced more quickly than C_0 , so θ_{\max}/C_0 decreases with downstream distance.

This argument suggests that as one goes downstream from the source, θ_{\max}/C_0 first increases, reaches a maximum, and then decreases.

A.1.2. *Cross-stream variations*

Near the source, since diffusion acts relatively slowly, we expect θ_{\max} to decrease slowly away from the centreline, i.e. on a length scale larger than L .

Far downstream the argument in the previous subsection suggests that θ_{\max} decreases rapidly relative to C_0 . But at this point the cross-stream profile of θ_{\max} is already much wider than L . Far from the centreline the relative difference in time scales will probably set in earlier than on the centreline, so the far fringes of the θ_{\max}

profile will be reduced relative to the C profile, and the widths of the θ_{\max} and C profiles will gradually get closer. This is consistent with our argument in §2.3, which suggested that very far downwind $\theta_{\max} \sim C$.

A.2. The effect of varying Pe and Re

A.2.1. Varying κ with fixed v , u and l

Near the source, increasing κ (i.e. decreasing Pe) gives smaller T_D without affecting T_A . Thus we expect smaller θ_{\max} , with unchanged C_0 , i.e. smaller θ_{\max}/C_0 .

Far from the source, T_D and T_A are unaffected, but larger κ gives smaller θ_{\max}/C_0 because of the near-source effect.

A.2.2. Varying u with fixed κ , v and l

Near the source, larger u (i.e. larger Pe and Re) will give larger L and, hence, smaller C_0 . Thus T_D will also be larger, giving larger θ_{\max} , so θ_{\max}/C_0 is larger.

Far from the source, larger u gives smaller T_A and larger ϵ , and hence smaller T_D . But $T_D/T_A \propto Re^{-1/2}$ is smaller, so θ_{\max}/C_0 decreases faster. However, as a result of the near-source behaviour θ_{\max}/C_0 starts out larger in this regime, so, except possibly very far downstream, we expect larger θ_{\max}/C_0 .

A.2.3. Varying l with fixed κ , v and u

Near the source, larger l (i.e. larger Pe and Re) gives larger L and thus larger T_D , T_A and T_D/T_A . So θ_{\max}/C_0 will be larger.

Far from the source, larger l gives larger T_D and T_A , and smaller $T_D/T_A \propto Re^{-1/2}$. So θ_{\max}/C_0 decreases more rapidly, but starting from a larger value. So we expect θ_{\max}/C_0 to be larger, except possibly very far downstream.

A.2.4. Varying v with fixed κ , u and l

Larger v (i.e. smaller Re) gives smaller T_D far from the source, without affecting any of the other time scales. So we expect smaller θ_{\max}/C_0 far from the source.

A.2.5. Conclusions

The general picture is one where increasing Pe and/or Re will tend to increase θ_{\max}/C_0 . But the precise relationship seems uncertain, and it will probably also depend on parameters like L_0/λ_C .

REFERENCES

- ANAND, M. S. & POPE, S. B. 1985 Diffusion behind a line source in grid turbulence. In *Turbulent Shear Flows 4* (ed. L. J. S. Bradbury *et al.*), pp. 46–61. Springer.
- ANDERSON, C. W., MOLE, N. & NADARAJAH, S. 1997 A switching Poisson process model for high concentrations in short-range atmospheric dispersion. *Atmos. Environ.* **31**, 813–824.
- BATCHELOR, G. K. 1949 Diffusion in a field of homogeneous turbulence. Part I. Eulerian analysis. *Austral. J. Sci. Res.* **2**, 437–450.
- BATCHELOR, G. K. 1952 The effect of homogeneous turbulence on material lines and surfaces. *Proc. R. Soc. Lond. A* **213**, 349–366.
- BATCHELOR, G. K. 1959 Small-scale variation of convected quantities like temperature in turbulent fluid. Part 1. General discussion and the case of small conductivity. *J. Fluid Mech.* **5**, 113–133.
- BUCH, K. A. & DAHM, W. J. A. 1996 Experimental study of the fine scale structure of conserved scalar mixing in turbulent shear flows. Part 1. $Sc \gg 1$. *J. Fluid Mech.* **317**, 21–71.
- BUCH, K. A. & DAHM, W. J. A. 1998 Experimental study of the fine-scale structure of conserved scalar mixing in turbulent shear flows. Part 2. $Sc \approx 1$. *J. Fluid Mech.* **364**, 1–29.
- CHATWIN, P. C. & ROBINSON, C. 1997 The moments of the pdf of concentration for gas clouds in the presence of fences. *Il Nuovo Cimento* **20 C**, 361–383.

- CHATWIN, P. C. & SULLIVAN, P. J. 1979 The relative diffusion of a cloud of passive contaminant in incompressible turbulent flow. *J. Fluid Mech.* **91**, 337–355.
- CHATWIN, P. C. & SULLIVAN, P. J. 1990a A simple and unifying physical interpretation of scalar fluctuation measurements from many turbulent shear flows. *J. Fluid Mech.* **212**, 533–556.
- CHATWIN, P. C. & SULLIVAN, P. J. 1990b Cloud-average concentration statistics. *Math. Computers Sim.* **32**, 49–57.
- CLARKE, L. & MOLE, N. 1995 Modelling the evolution of moments of contaminant concentration in turbulent flows. *Environmetrics* **6**, 607–617.
- CONTROL OF SUBSTANCES HAZARDOUS TO HEALTH REGULATIONS 2002 Statutory Instrument 2002 No. 2677, HMSO.
- CORRIVEAU, A. F. & BAINES, W. D. 1993 Diffusive mixing in turbulent jets as revealed by a pH indicator. *Exps. Fluids* **16**, 129–136.
- DAHM, W. J. A., SOUTHERLAND, K. B. & BUCH, K. A. 1991 Direct, high resolution, four-dimensional measurements of the fine scale structure of $Sc \gg 1$ molecular mixing in turbulent flows. *Phys. Fluids A* **3**, 1115–1127.
- DAVIES, J. K. W. 1989 The application of box models in the analysis of toxic hazards by using the probit dose-response relationship. *J. Haza. Mater.* **22**, 319–329.
- DERKSEN, R. W. & SULLIVAN, P. J. 1990 Moment approximations for probability density functions. *Combust. Flame* **81**, 378–391.
- GRIFFITHS, R. F. 1991 The use of probit expressions in the assessment of acute population impact of toxic releases. *J. Loss Prev. Process Ind.* **4**, 49–57.
- KRISTENSEN, L., WEIL, J. C. & WYNGAARD, J. C. 1989 Recurrence of high concentration values in a diffusing, fluctuating scalar field. *Boundary-Layer Met.* **47**, 263–276.
- LABROPULU, F. & SULLIVAN, P. J. 1995 Mean-square values of concentration in a contaminant cloud. *Environmetrics* **6**, 619–625.
- LEWIS, D. M. & CHATWIN, P. C. 1995a The treatment of atmospheric dispersion data in the presence of noise and baseline drift. *Boundary-Layer Met.* **72**, 53–85.
- LEWIS, D. M. & CHATWIN, P. C. 1995b A new model PDF for contaminants dispersing in the atmosphere. *Environmetrics* **6**, 583–593.
- LEWIS, D. M. & CHATWIN, P. C. 1997 A three-parameter PDF for the concentration of an atmospheric pollutant. *J. Appl. Met.* **36**, 1064–1075.
- LEWIS, D. M., CHATWIN, P. C. & MOLE, N. 1997 Investigation of the collapse of the skewness and kurtosis exhibited in atmospheric dispersion data. *Il Nuovo Cimento* **20 C**, 385–398.
- MOLE, N. 1995 The α - β model for concentration moments in turbulent flows. *Environmetrics* **6**, 559–569.
- MOLE, N. 2001 The large time behaviour in a model for concentration fluctuations in turbulent dispersion. *Atmos. Environ.* **35**, 833–844.
- MOLE, N., ANDERSON, C. W., NADARAJAH, S. & WRIGHT, C. 1995 A generalized Pareto distribution model for high concentrations in short-range atmospheric dispersion. *Environmetrics* **6**, 595–606.
- MOLE, N. & CLARKE, E. D. 1995 Relationships between higher moments of concentration and of dose in turbulent dispersion. *Boundary-Layer Met.* **73**, 35–52.
- MOSELEY, D. J. 1991 A closure hypothesis for contaminant fluctuations in turbulent flow. MSc thesis, University of Western Ontario, London.
- MUNRO, R. J., CHATWIN, P. C. & MOLE, N. 2001 The high concentration tails of the probability density function of a dispersing scalar in the atmosphere. *Boundary-Layer Met.* **98**, 315–339.
- MUNRO, R. J., CHATWIN, P. C. & MOLE, N. 2003a A concentration pdf for the relative dispersion of a contaminant plume in the atmosphere. *Boundary-Layer Met.* **106**, 411–436.
- MUNRO, R. J., CHATWIN, P. C. & MOLE, N. 2003b Some simple statistical models for relative and absolute dispersion. *Boundary-Layer Met.* **107**, 253–271.
- MYLNE, K. R. & MASON, P. J. 1991 Concentration fluctuation measurements in a dispersing plume at a range of up to 1000 m. *Q. J. R. Met. Soc.* **117**, 177–206.
- PICKANDS, J. 1975 Statistical inference using extreme order statistics. *Ann. Statist.* **3**, 119–131.
- POPE, S. B. 2000 *Turbulent Flows*. Cambridge University Press.
- SAWFORD, B. L. 2004 Micro-mixing modelling of scalar fluctuations for plumes in homogeneous turbulence. *Flow, Turb. and Combust.* **72**, 133–160.

- SAWFORD, B. L. & SULLIVAN, P. J. 1995 A simple representation of a developing contaminant concentration field. *J. Fluid Mech.* **289**, 141–157.
- SAWFORD, B. L. & TIVENDALE, C. M. 1992 Measurements of concentration statistics downstream of a line source in grid turbulence. In *Proc. 11th Australasian Fluid Mechanics Conf.*, Hobart, 14–18 Dec. 1992. University of Tasmania.
- SCHOPFLOCHER, T. P. 2001 An examination of the right-tail of the PDF of a diffusing scalar in a turbulent flow. *Environmetrics* **12**, 131–145.
- SCHOPFLOCHER, T. P., SMITH, C. J. & SULLIVAN, P. J. 2007 Scalar concentration reduction in a contaminant cloud. *Boundary-Layer Met.* **122**, 683–700.
- SCHOPFLOCHER, T. P. & SULLIVAN, P. J. 2002 A mixture model for the PDF of a diffusing scalar in a turbulent flow. *Atmos. Environ.* **36**, 4405–4417.
- SCHOPFLOCHER, T. P. & SULLIVAN, P. J. 2005 The relationship between skewness and kurtosis of a diffusing scalar. *Boundary-Layer Met.* **115**, 341–358.
- STAPOUNTZIS, H., SAWFORD, B. L., HUNT, J. C. R. & BRITTER, R. E. 1986 Structure of the temperature field downwind of a line source in grid turbulence. *J. Fluid Mech.* **165**, 401–424.
- TEN BERGE, W. F., ZWART, A. & APPELMAN, L. M. 1986 Concentration-time mortality response relationship of irritant and systemically acting vapours and gases. *J. Haza. Mater.* **13**, 301–309.
- WARHAFT, Z. 1984 The interference of thermal fields from line sources in grid turbulence. *J. Fluid Mech.* **144**, 363–387.
- YE, H. 1995 A new statistic for the contaminant dilution process in turbulent flows. PhD thesis, University of Western Ontario, London.
- XIE, Z.-T., HAYDEN, P., ROBINS, A. G. & VOKE, P. R. 2007 Modelling extreme concentrations from a source in a turbulent flow over a rough wall. *Atmos. Environ.* **41**, 3395–3406.